

Three-dimensional epitaxy: Thermodynamic stability range of coherent germanium nanocrystallites in silicon

S. Balasubramanian,^{a)} G. Ceder, and K. D. Kolenbrander

Department of Materials Science and Engineering, Massachusetts Institute of Technology, Cambridge, Massachusetts 02139

(Received 12 October 1995; accepted for publication 2 January 1996)

We study the stability range of coherent Ge quantum dots with an epitaxial Si shell. The critical radius is evaluated as a function of Si shell thickness and Ge nanocrystallite radius by comparing the energy of the system in the coherent and incoherent state. We find that the system is coherent up to a Ge nanocrystallite radius of about 100 Å, irrespective of the Si shell thickness. Nanocrystallites of radii larger than 270 Å lose coherency by the generation of perfect dislocation loops. In nanocrystallites of intermediate radii (between 100 and 270 Å), the coherency is lost by the introduction of partial dislocation loops enclosing a stacking fault. As the shell thickness decreases, the critical radius increases. © 1996 American Institute of Physics. [S0021-8979(96)00108-0]

I. INTRODUCTION

One-dimensionally quantum confined semiconductor thin films (“quantum well”) structures have emerged as important materials systems in today’s microelectronic and optoelectronic technologies. These lattice mismatched thin film heterostructures rely on the difference in band gap of the semiconductors to attain quantum confinement. A critical factor in the technological success of these strained layer epitaxial systems lies in the ability to grow coherent interfaces without defects, as these defects are generally detrimental to electrical and optical properties.

Theoretical treatments to describe the epitaxial relationships observed on mismatched thin film systems are well developed. This extensive literature builds on the pioneering efforts of Frank and van der Merwe,^{1–6} and Jesser and Matthews^{7–9} who predicted that a coherent epilayer of a crystal can be grown on a substrate of different lattice parameter. A direct result of these efforts is the community’s present understanding of the concept of a “critical thickness” that defines the maximum size at which the misfitting layer remains coherent with the host matrix.

Recently, experimental advances in materials processing have permitted the fabrication of three-dimensionally quantum confined semiconductor nanocrystallite (“quantum dot”) systems positioned within semiconductor host materials.^{10–12} In particular, Ge nanocrystallites have been synthesized by pulsed laser ablation and subsequently codeposited into a Si host grown by chemical beam epitaxy using disilane.¹³ These materials represent the three-dimensionally confined analogs to quantum well heterostructures. As with quantum wells, lattice coherency at the dot/host interface holds a key in defining the electronic, optoelectronic, and photonic characteristics of these heterostructures. A theoretical understanding of the morphological limits of three-dimensional epitaxy in these systems is needed to accompany the experimental efforts as the promise of quantum dot materials is further explored. An appropriate first step is the determination of a “critical radius” that describes the largest

sphere that can be coherently supported in a mismatched system of nanocrystallite and host.

Although nanocrystallite structures have to date not been studied from a point of view of coherency, the conditions under which a precipitate is coherent with its matrix has been known by the metallurgical community for many decades. In 1940, Nabarro^{14,15} determined the elastic strains developed when a precipitate is formed in an alloy. Nabarro,¹⁵ Jesser,¹⁶ Brown^{17,18} and others calculated the critical size of precipitates. Brown¹⁷ considered the interaction of one dislocation with coherent spherical precipitates and evaluated the critical size from a thermodynamic point of view.

We present here the first effort to describe the critical limits of epitaxy for three-dimensionally confined nanocrystallites in a crystalline host. Building simultaneously on the principles of the quantum well strained layer epitaxy and on the understanding of coherent precipitates in alloys, we have calculated the critical radius of a semiconductor of different lattice parameter. We choose as our representative system the epitaxial positioning of Ge nanocrystallites in a crystalline Si host.

II. THERMODYNAMIC CONSIDERATIONS

The lattice parameter of bulk Ge is approximately 4% larger than that of Si. When a thick Si shell is grown epitaxially on a Ge nanocrystallite of bulk lattice parameter, the lattice misfit causes coherency strains to develop in the system. As the radius of the nanocrystallite increases, the stress increases and reaches a stage where the misfit strain can no longer be accommodated coherently. At this point coherency is lost by the formation of defects (i.e., dislocations) and the system transforms to an incoherent state.

The coherent-to-incoherent transformation becomes thermodynamically favorable if the total energy of the system after transformation is less than the total energy before transformation, i.e., $E_{\text{Incoherent}} \leq E_{\text{Coherent}}$. However, this is not the only requirement for this transformation to take place as the nucleation kinetics of the defect may play an important role. In planar epitaxy it is found that dislocation-free interfaces can be grown upto a film thicknesses 5–10 times

^{a)}Electronic mail: shuba@mit.edu

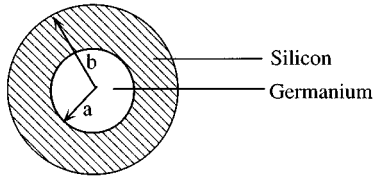


FIG. 1. Schematic diagram: Ge nanocrystallite capped with Si shell.

larger than the critical thickness predicted by Matthews^{19,20} and Van der Merwe^{1,6}. This metastability in the system has been explained by the slow kinetics of the system and/or the insensitivity of the experimental techniques used.²¹ The thermodynamic critical radius which is determined in this paper can, therefore, be seen as the minimal radius at which Si capped Ge particles can be kept coherent.

At the critical radius, the energy of the system in the coherent state and incoherent state are equal. In the coherent state, the energy of the system is the elastic strain energy caused by the misfit,

$$E_{\text{Coherent}} = E_{\text{Elastic}} \quad (1)$$

In the incoherent state the stress field of the defect interacts with the stress field of the misfitting nanocrystallite and relieves part of the misfit strain, thereby releasing a part of the elastic strain energy, leaving a residual elastic energy. In addition, energy is required to create the defect. Therefore, the energy of the system in the incoherent state is

$$E_{\text{Incoherent}} = E_{\text{Residual Elastic}} + E_{\text{Defect}} \quad (2)$$

In calculating these energy contributions, we assume that both nanocrystallite and shell materials are elastically isotropic and that the laws of continuum mechanics are applicable to the nanocrystallite/shell systems.

A. Coherent state

1. Elastic strain energy

We assume that the spherical Ge nanocrystallite is epitaxially capped with a concentric Si shell having the same orientation as the nanocrystallite. A schematic diagram of the system is shown in Fig. 1. The inner region, $0 < r < a$, is the Ge nanocrystallite and the outer region $a < r < b$ is the Si shell. We consider a range of Si shell thicknesses, $t = (b - a)$, ranging from 0 to infinity, and evaluate the critical radius as a function of Ge nanocrystallite radius and Si shell thickness.

The total elastic strain energy is the elastic strain energy stored both in the germanium nanocrystallite and the Si shell, which can be computed from the stress and strain fields.

The system possesses spherical symmetry and the displacements and fields are only a function of the radial coordinate r . The misfitting Ge nanocrystallite produces a tensile stress on the interface, while the outer surface of the Si shell is traction free.

The stress and strain fields inside the spherical germanium nanocrystallite are purely hydrostatic. The hydrostatic stress component is the interface pressure, p , between the Ge nanocrystallite and the Si shell:

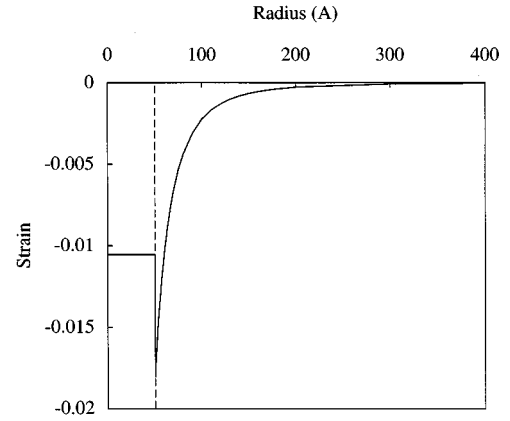


FIG. 2. Radial strain field for a 50 Å Ge nanocrystallite with a 350 Å thick Si shell.

$$\sigma_{rr}^{\text{Ge}} = \sigma_{\theta\theta}^{\text{Ge}} = \sigma_{\phi\phi}^{\text{Ge}} = -p \quad (3)$$

For a stress free outer boundary this interface pressure is given by²²

$$p = \frac{\frac{2E_{\text{Si}}}{3(1-\nu_{\text{Si}})} \epsilon(1-c)}{1 - \frac{2m}{3}(1-c)} \quad (4)$$

where E_{Si} is the Young's modulus of Si, ν_{Si} is the Poisson's ratio of Si, $c = a^3/b^3$ is the volume fraction of the nanocrystallite, $m = E_{\text{Si}}/(1-\nu_{\text{Si}})[(1-2\nu_{\text{Si}})/E_{\text{Si}} - (1-\nu_{\text{Ge}})/E_{\text{Ge}}]$ is the elastic mismatch parameter, and $\epsilon = [3K_{\text{Ge}}/(3K_{\text{Ge}} + 4\mu_{\text{Si}})] \times [(a_{\text{Ge}} - a_{\text{Si}})/a_{\text{Si}}]$ is the constrained strain for a spherical geometry as defined by Eshelby²³ and Nabarro,¹⁴ K_{Ge} is the Bulk modulus of Ge and μ_{Si} the shear modulus of Si. The constrained strain is calculated assuming that the lattice parameter of the nanocrystallite is the same as in bulk.

The stress and strain fields in the silicon shell vary according to the distance from the center of the nanocrystallite:²⁴

$$\sigma_{rr}^{\text{Si}} = \frac{cp}{(1-c)} \left[1 - \left(\frac{b}{r}\right)^3 \right], \quad (5)$$

$$\sigma_{\theta\theta}^{\text{Si}} = \sigma_{\phi\phi}^{\text{Si}} = \frac{cp}{(1-c)} \left[1 + \frac{1}{2} \left(\frac{b}{r}\right)^3 \right]. \quad (6)$$

The radial and tangential components of the strain fields (for a 50 Å Ge nanocrystallite with a 350 Å thick Si shell) are shown in Figs. 2 and 3 respectively.

For the system considered, the elastic strain energy is

$$E_{\text{Elastic}} = \frac{1}{2}(3\sigma_{rr}^{\text{Ge}}e_{rr}^{\text{Ge}})\left(\frac{4}{3}\pi a^3\right) + \frac{1}{2} \int_b^a (\sigma_{rr}^{\text{Si}}e_{rr}^{\text{Si}} + 2\sigma_{\theta\theta}^{\text{Si}}e_{\theta\theta}^{\text{Si}})(4\pi r^2 dr) \quad (7)$$

where the first term is due to the Ge nanocrystallite and the second term is due to the Si shell. Upon substitution of the relevant terms it simplifies to

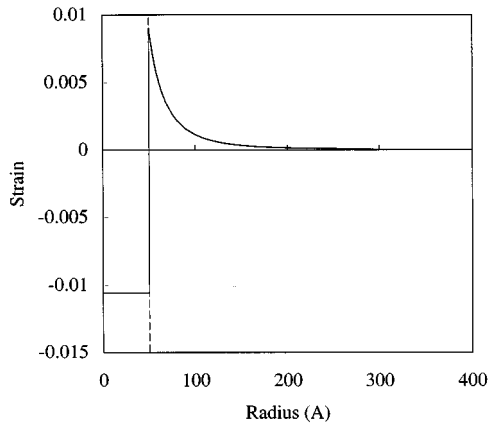


FIG. 3. Tangential strain field for a 50 Å Ge nanocrystallite with a 350 Å thick Si shell.

$$E_{\text{Elastic}} = \left(\pi a^3 p^2 \right) \left[\frac{1-2\nu_{\text{Ge}}}{1+\nu_{\text{Ge}}} \frac{1}{\mu_{\text{Ge}}} + \frac{1-2\nu_{\text{Si}}}{1+\nu_{\text{Si}}} \frac{1}{\mu_{\text{Si}}} \frac{c}{(1-c)} + \frac{1}{2\mu_{\text{Si}}(1-c)} \right]. \quad (8)$$

B. Incoherent state

The interface between the Ge nanocrystallite and the Si shell can become incoherent when the introduction of interfacial defects lowers the energy of the system.

1. Defect energy

Our predictions of critical radius of the Ge nanocrystallite will depend on our judicious choice of the possible incoherency defects. We consider both strain relief by a perfect dislocation loop and by a stacking fault bounded by a partial dislocation loop. It is reasonable to assume that a dislocation loop is preferred over a set of dislocations that terminate at the surface.

To determine the dislocation energy we assume, that the energy required to create the dislocation loop in a finite medium is the same as the energy required to create the dislocation in an infinite medium. This assumption is valid until the shell thickness becomes so small that the dislocation interacts with the free surface.

The energy to create a circular dislocation loop in an infinite medium, with Burgers vector perpendicular to the plane of the loop is calculated by approximating the true dislocation configuration by piece wise straight configurations. Each segment of the loop is acted upon by a force caused by the stress originating from all other parts of the loop, and the work done against all these forces is the work done to create the dislocation loop. Thus, the interaction energy between all segments of loop (approximated into a piece wise-straight configuration) can be calculated accurately as²⁵

$$E_{\text{Loop}} = 2\pi r_{\text{loop}} \left(\frac{\mu |b|^2}{4\pi(1-\nu)} \right) \ln \left(\frac{8\alpha r_{\text{loop}}}{|b|} - 1 \right) \quad (9)$$

where α is the dislocation core parameter, r_{loop} is the radius of the dislocation loop, and $|b|$ is the burgers vector of the dislocation loop.

a. Perfect dislocation loops. We assume the dislocations to be vacancy-type prismatic dislocation loops with burgers vector ($|b| = 1/2\langle 110 \rangle$) perpendicular to the plane of the loop. The dislocation loop is assumed to be at the interface between the Ge nanocrystallite and the Si shell. Further, the radius of the dislocation loop is assumed to be the radius of the Ge nanocrystallite.

As the dislocation loop is created at the interface between the Ge nanocrystallite and the Si shell, we use the average shear modulus of the interface²⁶ $\mu_{\text{interface}} = 2\mu_{\text{Si}}\mu_{\text{Ge}}/(\mu_{\text{Si}} + \mu_{\text{Ge}})$ in Eq. (9).

The defect energy in Eq. (2) for this defect is the energy of the dislocation loop.

b. Partial dislocations enclosing a stacking fault. An alternate mechanism for strain relief is assumed to be by a Frank partial dislocation loop with burgers vector ($|b| = \frac{1}{3}\langle 111 \rangle$) bounding an intrinsic stacking fault. The energy required to create this partial loop is given by Eq. (9), and the energy to create the intrinsic stacking fault is

$$E_{\text{Stacking Fault}} = \pi r_{\text{loop}}^2 \gamma \quad (10)$$

where γ is the stacking fault energy of Ge. The defect energy in Eq. (2) for this defect is

$$E_{\text{Defect}} = E_{\text{Loop}} + E_{\text{Stacking Fault}} \quad (11)$$

2. Residual elastic energy

The stress field of the dislocation relieves part of the strain in the misfitting system. The energy released by loop formation (interaction energy) is evaluated without using explicit expressions for the field of the dislocation, following the general procedure outlined by Eshelby,²³

$$E_{\text{Interaction}} = \pi r_{\text{loop}}^2 p |b| \quad (12)$$

where r_{loop} is the radius of the dislocation loop formed at the interface between the Ge nanocrystallite and the Si shell, p the interface pressure as defined in Eq. (9) and $|b|$ is the Burgers vector of the loop formed. In the case of partial dislocation enclosing a stacking fault, there is no strain relief by the stacking fault and all the strain relief is by the partial dislocation.

The contribution of this strain relieving mechanism to the residual elastic energy of the system can be considered by subtracting the interaction energy from the elastic energy:

$$E_{\text{Residual Elastic}} = E_{\text{Elastic}} - E_{\text{Interaction}} \quad (13)$$

III. RESULTS AND DISCUSSION

In calculating the energies of the states to estimate the critical radius, we use the following values for the parameters: $\mu_{\text{Si}} = 66.6$ GPa, $E_{\text{Si}} = 162.9$ GPa, $\nu_{\text{Si}} = 0.22$, $\mu_{\text{Ge}} = 54.6$ GPa, $E_{\text{Ge}} = 132.8$ GPa, $\nu_{\text{Ge}} = 0.21$ (Ref. 27), $\gamma_{\text{Ge}} = 60$ mJ/m² (Ref. 28), $\alpha = 4$ (Ref. 29).

Figure 4 shows the critical radius of the Ge nanocrystallite as a function of the Si shell thickness. We find that, for very thick Si shells (>1000 Å), the Ge–Si interface remains

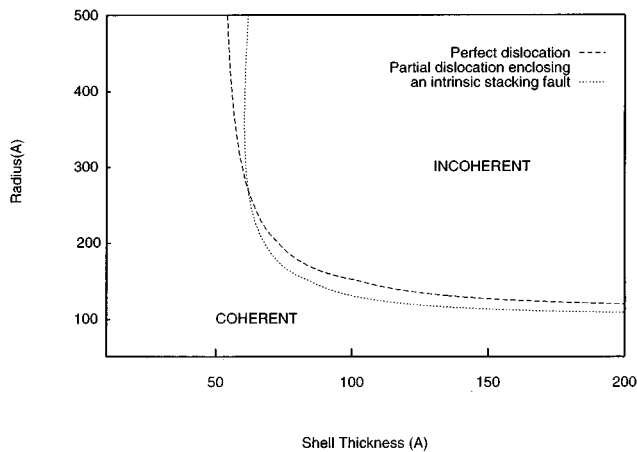


FIG. 4. Contour of critical radius as a function of Si shell thickness and Ge nanocrystallite radius.

coherent up to a Ge nanocrystallite radius of 100 Å. The critical radius of the Ge nanocrystallite in a very thick shell is found to be approximately three times the critical thickness of a Ge film on an infinite Si substrate. This can be explained in terms of the interface area to volume ratio. For a given volume of Ge nanocrystallite or film, the interface area between the spherical nanocrystallite and the Si matrix is less than the interface area between the Ge film and Si substrate. Therefore, the strain relief provided by introducing dislocations for the Ge nanocrystallite is smaller than for the Ge film of the equal volume. Hence generating dislocations in a nanocrystallite becomes less favorable until much larger radii.

For a thinner Si shell, the critical radius of the Ge nanocrystallite increases significantly as the total strain energy of the system decreases. As the Ge nanocrystallite radius increases, it becomes energetically less favorable to create partial dislocations enclosing stacking faults at a Ge nanocrystallite radius of greater than 270 Å. Therefore, coherency is lost by forming a perfect dislocation loop rather than creating a partial dislocation loop enclosing a stacking fault.

We now assess the validity of the approximations made in our calculations. At very small shell thicknesses, the energy required to create the dislocation in a finite medium is not equal to that in an infinite medium. The effect of the free surface on the dislocation loop has to be considered in evaluating the energy required to generate the dislocation. This interaction between the dislocation and the free surface decreases the energy of the system in the incoherent state, hence the critical radius for systems with very small shell thickness will be lower than what we have estimated.

The values used for the parameters in these calculations are approximate. We tested the sensitivity of our results on the value used for the parameters.

In evaluating the energy required to create a dislocation loop (perfect or partial) we use a dislocation core parameter, α , of 4 (Ref. 29), which is typical for diamond cubic materials. However, other values ranging between 1 and 5 have been used in the literature. Therefore, the critical radius is also evaluated as a function of dislocation core parameter at

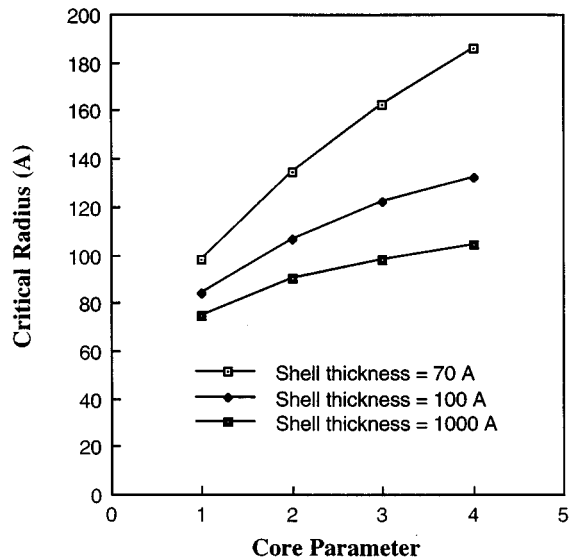


FIG. 5. Variation of the critical radius as a function of the core parameter of the partial dislocations.

various shell thicknesses, as shown in Fig. 5. The critical radius is found to vary substantially with the core parameter α . The effect of dislocation core parameter on the critical radius is more pronounced at smaller Si shell thicknesses.

In evaluating the energy required to create an intrinsic stacking fault, we use a Ge stacking fault energy of 60 mJ/m². However, there remains some disagreement in measurements of stacking fault energies in Ge. Intrinsic stacking fault energies of 30 mJ/m² (Ref. 30) and 60 mJ/m² (Ref. 28) have been reported in literature. The critical radius is evaluated as a function of stacking fault energy at various shell thicknesses, as shown in Fig. 6. The critical radius is found

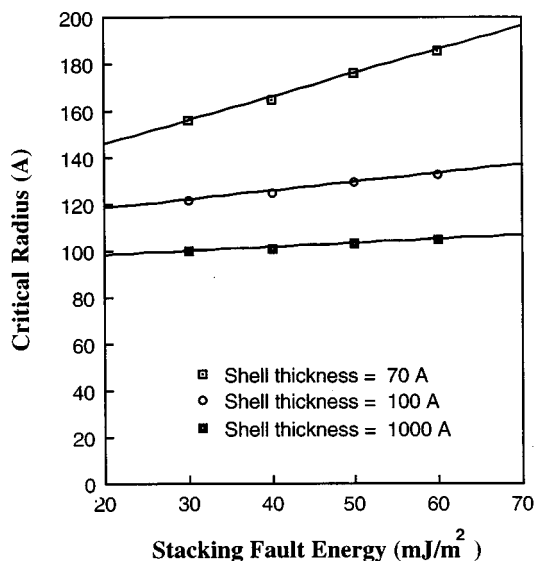


FIG. 6. Effect of stacking fault energy on the critical radius.

to increase as the stacking fault energy increases. The effect of stacking fault energy on the critical radius is more pronounced at smaller Si shell thicknesses.

The interaction energy (energy released by loop formation) can at most be equal to the elastic strain energy of the system. In our model, this condition is satisfied only for Ge nanocrystallites with radii greater than 20 Å, limiting the applicability of this method.

IV. CONCLUSIONS

The system is coherent up to a Ge nanocrystallite radius of about 100 Å, irrespective of the Si shell thickness. Nanocrystallite of radii larger than 270 Å lose coherency by the generation of perfect dislocation loops. For intermediate Ge nanocrystallite radii (between 100 and 270 Å), the coherency is lost by the introduction of partial dislocation loops enclosing a stacking fault. As the shell thickness decreases, the critical radius increases.

The significant effect of the stacking fault energy and dislocation core parameter on the critical radius is found to be more significant at smaller shell thicknesses, indicating the approximate nature of these calculations. Typical nanocrystallite radii of experimental interest are of the order of 50 Å or less. Therefore, we conclude that extremely large Ge nanocrystallites capped with Si shells can be grown without producing dislocations. We view this as an important determination in our efforts to experimentally grow these structures.

ACKNOWLEDGMENTS

We thank Professor R. W. Balluffi, Dr. M. K. Aydinol and Mr. P. D. Tepesch for helpful discussions. Authors S. B. and K. D. K acknowledge support from National Science Foundation under Contract No. DMR-9258554 and G. C. acknowledges support from the National Science Foundation under Contract No. DMR-9501856.

¹F. Frank and J. van der Merwe, Proc. R. Soc. London Ser. A **198**, 205 (1949).

- ²F. Frank and J. van der Merwe, Proc. R. Soc. London Ser. A **198**, 216 (1949).
- ³F. Frank and J. van der Merwe, Proc. R. Soc. London Ser. A **200**, 125 (1949).
- ⁴F. Frank and J. van der Merwe, Proc. R. Soc. London Ser. A **201**, 261 (1949).
- ⁵J. van der Merwe, J. Appl. Phys. **34**, 117 (1963).
- ⁶J. van der Merwe, J. Appl. Phys. **34**, 123 (1963).
- ⁷J. Matthews and W. Jesser, Philos. Mag. **15**, 1097 (1967).
- ⁸J. Matthews and W. Jesser, Philos. Mag. **17**, 461 (1968).
- ⁹J. Matthews and W. Jesser, Philos. Mag. **17**, 595 (1968).
- ¹⁰S.-T. Ngiam, K. Jensen, and K. D. Kolenbrander, in *Growth, Processing and Characterization of Semiconductor Heterostructures*, edited by G. Gumbs, S. Luryi, B. Weiss, and G. Wicks (Materials Research Society Symposium Proceedings, Boston, 1994), Vol. 326, p. 263.
- ¹¹M. Danek, K. Jensen, C. Murray, and M. Bawendi, Appl. Phys. Lett. **65**, 2795 (1994).
- ¹²M. Danek, K. Jensen, C. Murray, and M. Bawendi, in *Growth, Processing and Characterization of Semiconductor Heterostructures*, edited by G. Gumbs, S. Luryi, B. Weiss, and G. Wicks, Materials Research Society Symposium Proceedings, Vol. 326 (Materials Research Society, Boston, 1994), p. 275.
- ¹³S.-T. Ngiam, K. Jensen, and K. D. Kolenbrander, J. Appl. Phys. **76**, 8201 (1994).
- ¹⁴N. Mott and F. Nabarro, Proc. Phys. Soc. **52**, 86 (1940).
- ¹⁵F. Nabarro, Proc. R. Soc. London Ser. A **175**, 519 (1940).
- ¹⁶W. Jesser, Philos. Mag. **19**, 993 (1969).
- ¹⁷L. Brown, G. Woolhouse, and U. Valdre, Philos. Mag. **17**, 781 (1967).
- ¹⁸L. Brown, Philos. Mag. **10**, 441 (1964).
- ¹⁹J. Matthews, J. Vac. Sci. Technol. **12**, 126 (1975).
- ²⁰J. Matthews, S. Mader, and T. Light, J. Appl. Phys. **41**, 3800 (1970).
- ²¹D. Houghton, D. Perovic, J.-M. Baribeau, and G. Weatherly, J. Appl. Phys. **67**, 1850 (1990).
- ²²S. Suresh, A. Giannakopoulos, and M. Olsson, J. Mech. Phys. Solids **V42**, 979 (1994).
- ²³J. Eshelby, Proc. R. Soc. London Ser. A **241**, 376 (1957).
- ²⁴W. Lai, D. Rubin, and E. Krempl, *Introduction to Continuum Mechanics* (Pergamon, New York, 1993).
- ²⁵J. Hirth and J. Lothe, *Theory of Dislocations* (Wiley, New York, 1982).
- ²⁶J. Matthews, *Epitaxial Growth* (Academic, New York, 1975), Part B.
- ²⁷G. Simmons and H. Wang, *Single Crystal Elastic Constants*, 2nd ed. (MIT, Cambridge, MA, 1971).
- ²⁸A. Gomez, D. Cockayne, P. Hirsch, and V. Vitek, Philos. Mag. **31**, 105 (1975).
- ²⁹E. Fitzgerald, Mater. Sci. Rep. **7**, 87 (1991).
- ³⁰H. Foll and C. Carter, Philos. Mag. **40**, 497 (1979).